ESTIMATION OF THE PERMEABILITY OF HYDROCARBON RESERVOIR SAMPLES USING INDUCED POLARIZATION (IP) AND NUCLEAR MAGNETIC RESONANCE (NMR) METHODS

Fatemeh Razavirad[1,2,3] (Fatima.rad1999@gmail.com)

Myriam Schmutz[2] (Myriam.Schmutz@ipb.fr)

Andrew Binley[3] (a.binley@lancaster.ac.uk)

[1] Yazd University, Mining and Metallurgical Engineering Department, Iran.

[2] EA4592 – Bordeaux INP- UBM, France.

[3] Lancaster Environmental Centre, Lancaster University, United Kingdom.

SHORT TITLE: PERMEABILITY ESTIMATION USING IP& NMR

Original paper date of submission: 10th November 2017

Revised 17th October 2018

ABSTRACT

A number of published models utilizing induced polarization (IP) and nuclear magnetic resonance (NMR) measurements for the estimation of permeability of hydrocarbon reservoir samples are evaluated. IP and NMR measurements were made on 30 samples (clean sands and sandstones) from a Persian Gulf hydrocarbon reservoir. The applicability of a mechanistic IP-permeability model and an empirical IP-permeability model recently proposed is assessed. The mechanistic model results in a broader range of permeability estimates than those measured for sand samples, while the empirical model tends to overestimate the permeability of the samples tested here. An NMR permeability prediction model that is based on porosity (ϕ) and the mean of log transverse relaxation time (T_{2ml}) is also evaluated. This model provides reasonable permeability estimations for clean sandstones tested here but relies on calibrated parameters. An IP-NMR permeability model, which is based on the peak of the transverse relaxation time distribution, T_{2p} and the formation factor, is also examined. This model consistently underestimates the permeability of the samples tested. A new model is then introduced.

This model estimates the permeability using the arithmetic mean of log transverse NMR relaxation time (T_{2ml}) and diffusion coefficient of the pore fluid. Using this model, estimates of permeability for both sandstones and sand samples is improved. This permeability model may offer a practical solution for geophysically-derived estimates of permeability in the field, although testing on a larger database of clean granular materials is needed.

INTRODUCTION

One of the oldest, yet still challenging, problems in hydrogeophysics is the prediction of permeability of rocks and soils aided by geophysical measurements (e.g. Dakhnov et al., 1967; Worthington and Collar, 1984). Permeability is one of the most important reservoir properties for designing and managing the recovery operation of hydrocarbon reservoirs, as it controls the flow of fluids inside the well during production. Consequently, with reliable estimates of permeability, oil reservoir engineers can

efficiently manage the production processes of a field. Fluid transport properties of porous media, including permeability, are also important for near-surface environmental applications, in particular for groundwater resource management. Conventional borehole-based hydraulic methods for estimating permeability are expensive and can often involve lengthy experimentation. Furthermore, such measurements can be limited to relatively small support volumes. Consequently, there has been much interest in the use of geophysical methods to assist in permeability estimation. Most notably, nuclear magnetic resonance (NMR) and induced polarization (IP) have received considerable attention.

Several studies have been carried out to predict the permeability using IP and spectral IP (SIP) methods (Börner et al., 1996; Sturrock et al., 1998, 1999; de Lima and Niwas, 2000; Slater and Lesmes, 2002). A number of studies have shown that the IP relaxation time is a relevant parameter for permeability estimation (Binley et al., 2005; Kemna et al., 2005; Zisser et al., 2010). Revil and Florsch (2010) proposed a mechanistic model for the prediction of the permeability of granular media. Their model is based on grain polarization expressed in terms of quadrature conductivity (σ''). In contrast, Revil et

al. (2012) established a link between IP relaxation time and pore size which allows an alternative permeability estimation approach. Revil et al. (2015) investigated such an approach using an extensive data sets including clean and clayey sands and sandstones; they found that the predicted permeability using this model is very close to the measured permeability for the samples tested. Weller et al. (2015), also working on an extensive database of IP measurements of sandstones and sands, developed empirically permeability estimation models and demonstrate reasonable predictive capability over a range of permeability values. Their models are based on two parameters including an electric substitute of effective porosity (the formation factor) and an electrical proxy of pore-normalized surface area (the imaginary part of electric conductivity).

The NMR method has been widely used to evaluate and characterize petroleum and water resources as it is the only geophysical method that can detect hydrogen directly. NMR measurements can be applied in both the laboratory (lab-NMR) and field including surface NMR (MRS) and borehole NMR (BNMR). MRS is a non-invasive method that is used to characterize aquifer materials (e.g., Hertrich, 2008; Legchenko et

al., 2002; Meju et al., 2002; Yaramanci et al., 1999). In the petroleum industry, BNMR is used to estimate water and hydrocarbon content, porosity and permeability of a reservoir (Banavar and Schwartz, 1987; Kleinberg et al., 1994; Allen et al., 2000). Longitudinal and transverse relaxation times (T_1 and T_2, respectively) of materials can be determined using laboratory-based NMR. In order to predict the permeability using NMR methods, a relationship is typically developed between the arithmetic mean of log relaxation times (T_{1ml} or T_{2ml}) and permeability (Coates et al., 1993; Straley et al., 1997; Kenyon, 1997). A number of studies have shown that the measured relaxation time is related to the surface area-to-volume ratio of the pore space (S_{por}) (e.g., Cohen and Mendelson, 1982; Keating and Knight, 2012) and so this relationship allows the use of NMR data to estimate pore sizes (e.g., Timur, 1969; Yaramanci et al., 2002) and permeability (e.g.,Vogeley and Moses, 1992; Legchenko et al., 2002).

There are a few studies that compare IP (or SIP) permeability models with NMR permeability models (Weller et al., 2010a; Weller et al., 2014; Osterman et al., 2016). Osterman et al. (2016) studied 45 sandstones cores collected from 15 different formations

with a broad range of permeability. They used the Katz and Thompson permeability model, which is based on the characteristic hydraulic length scale, determined from mercury injection capillary pressure (MICP), and the intrinsic formation factor, F. NMR measurements of the relaxation time associated with the peak of transverse relaxation time distribution (T_{2p}) and effective surface relaxivity (ρ_{2eff}) were used to estimate the hydraulic length scale and IP measurements were included to improve estimates of the formation factor. Surface relaxivity quantifies the ability of a surface to cause protons to relax, which is controlled by the strength of fluid-matrix interactions and the wettability of the rock surface (Coates et al., 1999). There is substantial experimental evidence that the surface relaxivity is a function of the concentration and mineralogy of paramagnetic species on the surface of the pore (Foley et al., 1996; Bryar et al., 2000; Keating and Knight, 2007, 2010). Therefore, Osterman et al. (2016) first determined the effective surface relaxivity (ρ_{2eff}) from a log-linear fit between pore-throat size (Λ) and the peak of transverse relaxation time distribution (T_{2p}). Based on the model of Osterman et al. (2016), permeability is proportional to the square of peak of transverse relaxation time distribution, T_{2p}^2 divided by formation factor, F.

This study builds on the growing literature examining geophysically derived permeability by evaluating electrical (IP) models and NMR models for the estimation of permeability specifically based on parameters measurable (in theory at least) from field geophysical surveys. Two models based on IP measurements (Revil and Florsch, 2010;Weller et al., 2015), one model based on NMR measurement (Kenyon et al., 1988) and one joint IP-NMR model (Osterman et al., 2016) are examined. Then, a new NMR model based on the widely known Katz and Thompson permeability model is derived. For the implementation of this model, the length scale is considered related to the NMR relaxation time and the diffusion coefficient of the saturating fluid; this length scale is then substituted into the Katz and Thompson permeability model, which is explained in detail later. Therefore, the current work builds on the work on Osterman et al. (2016) using a set of 30 reservoir samples, which includes eight sandstone plugs and 22 sand plugs, all with relatively high permeability. The main aim of this study is to assess the validity of current IP permeability models, NMR permeability models and IP-NMR models on clean granular materials typical of reservoir formations.

MATERIAL AND METHODS

In this study, relationships between hydraulic and electrical properties of 30 plug samples, which were provided by the Iranian Offshore Oil Company (a subsidiary of the National Iranian Oil Company), are investigated. All plugs used in this study were extracted from the original drill cores. The average length and diameter of each plug are 60 mm and 38 mm, respectively. The samples were obtained from depths between 2174 m and 2238 m in an oil field located in the Persian Gulf. The samples have high porosity and permeability (the average values of porosity and permeability of the investigated samples are 0.34 and 1.01×10^{-11} m^2, respectively).

Experimental procedure

A series of physical and petrophysical measurements were carried out on the plugs, as described below.

1) The grain size distribution was obtained by laser diffraction using a Mastersizer 2000 laser diffraction particle size analyzer.

2) The permeability of all samples was measured using air permeameter apparatus. Generally, pore size and their connectivity determine whether the porous medium has high or low permeability.

3) Sample porosity was determined gravimetrically. The core samples were weighed at saturation and after having been dried in an oven.

4) Cation exchange capacity (CEC) was obtained by measuring the quantity of a specific cation (in this case, sodium) that preferentially bonds to exchange sites. Sodium acetate was used as a sodium source and the displaced sodium measured using atomic absorption.

5) Pore surface area was measured using nitrogen gas adsorption, calculated using the 5 point BET (Brunauer et al., 1938). BET analysis provides precise specific surface area evaluation of materials by nitrogen multi-layer adsorption measured as a function of relative pressure using a fully automated analyzer. Pore surface area was

measured only on sand samples. Prior to the measurements, samples were dried. The mass of sample used for each measurement is approximately 5g.

6) The intrinsic formation factor was determined by resistivity measurements at several salinities using the model in equation **Error! Reference source not found.**. In this study we measured the formation factor by resistivity measurements over four different pore fluid salinities (100, 500, 1000 and 6000 mS/m).

SIP and NMR measurements were collected in a fully saturated state for each sample. All samples were saturated with a NaCl solution with an electric conductivity of 100 mS/m. The electrical impedance was measured using a four-point electrode array (see Figure 1a). The sample holder used in this study is similar that that designed by Binley et al. (2005), with slight modifications to the potential and current electrodes. Two silver coils were used as current electrodes to inject an alternating sinusoidal current (Figure 1b). The voltage and the phase shift between the applied current and measured voltage was determined using (In Vivo Metric, California) Ag-AgCl non-polarizing potential electrodes (Figure 1c). Electrical measurements were taken using the ZEL-SIP04-V02

impedance meter in a frequency range of 2 mHz to 45 kHz (Forschungszentrum Julich GmbH) (Zimmermann et al., 2008). Figure 1 shows the SIP experimental setup. The end caps were filled with the same fluid saturating the samples.

NMR data were collected using the ARTEC system (a low field NMR system) using a Carr-Purcell-Meiboom-Gill (CPMG) pulse sequence. The CPMG pulse sequence is a 90° pulse, followed by a series of refocusing 180° pulses, separated by the echo spacing.

Spectral Induced Polarization (SIP)

The complex conductivity (σ^*) of a porous medium is determined from measurements of the conductivity magnitude ($|\sigma|$) and phase shift (φ) between the injected current and measured potential. Complex conductivity includes two components: 1) the real part (σ'), which corresponds with the transport of free charges or conduction in the pore space; 2) the imaginary part (σ''), which is related to storage of charge or polarization in the pore space. The conductivity magnitude ($|\sigma|$) and phase shift (φ) can be written as follows:

$$|\sigma| = \sqrt{\sigma'^2 + \sigma''^2} \ , \tag{1}$$

$$\varphi = \tan^{-1}\left[\frac{\sigma''}{\sigma'}\right]. \quad (2)$$

In-phase conductivity (or electric conduction) (σ') in non-metallic rocks occurs through the pore-filling electrolyte (fluid) and by ionic migration in the electrical double layer (EDL) forming at the grain-fluid interface (Slater, 2007). The electrolyte conductivity (σ_{el}) and surface conductivity (σ'_{surf}) add in parallel (Vinegar and Waxman, 1984):

$$\sigma' = \sigma_{el} + \sigma'_{surf} = \left(\frac{1}{F}\right)(\sigma_f + \sigma'_{surf}), \quad (3)$$

where F is the electrical formation factor (unitless), σ_f is the conductivity of the pore-filling fluid (S/m) and σ'_{surf} is the surface conductivity (S/m).

Archie (1942) determined the electrical formation factor as a ratio between pore fluid conductivity (σ_f) and bulk conductivity (σ') for a saturated porous medium and stated that $F = \phi^{-m}$, where ϕ is the porosity and m is called the cementation exponent. This relationship is valid for a high salinity pore fluid. For low salinity pore fluid saturation or very high surface conductivity there is a significant difference between apparent and intrinsic formation factor, which can have a significant impact on permeability estimation

(Lesmes and Fridman, 2005) . The intrinsic formation factor can be determined from measurements at several salinities using an electrical conductivity model (by fitting the slope of equation 3) or estimated from a single salinity measurement using a relationship between the surface and quadrature conductivities (Weller et al., 2013) to compensate for surface conduction:

$$F' = \frac{\sigma_f}{\sigma' - (\sigma''/l)}\ , \tag{4}$$

where σ_f is pore fluid conductivity (0.1 S/m), σ' and σ'' are in-phase and quadrature conductivities at 1 Hz (S/m), respectively, and l=0.0421 (unitless), obtained by Weller et al. (2013) empirically.

Nuclear Magnetic Resonance (NMR)

Geophysical NMR methods exploit the magnetic dipole moment of hydrogen protons in water molecules. Any nuclei with an odd number of protons or neutrons or both (like the nucleus of hydrogen), due to their possession of a nuclear spin angular momentum, are suitable for NMR measurements (Coates et al., 1999). In an NMR

measurement, the nuclei expose to a static magnetic field, B_0 and then their nuclear spins align with the applied B_0. Therefore, the magnetic moments (M_0) of the hydrogen protons in the porous media is formed and then M_0 precess about the static magnetic field with Larmor frequency, $f = \frac{\gamma B_0}{2\pi}$, where γ is the gyromagnetic ratio, which is a measure of the strength of the nuclear magnetism. For hydrogen, $\frac{\lambda}{2\pi} = 42.58^{MHz}/_{T}$. Then, an oscillating magnetic field (B_1) perpendicular to the static field (B_0) is applied to the nuclei for a short time that it causes nuclei move away and after removing B_1, the nuclear spins relax back to their equilibrium positions. Then, the resonant EM field acquired by nuclei provides a measurable signal which is described in terms of two different types of relaxation times: longitudinal (T_1) and transverse (T_2) relaxations. In the recent literature, NMR relaxation in the porous media is well described (Bloch, 1946; Torrey, 1956). In this study, the transverse relaxation time (T_2), which is consistent with most NMR experimentation, is measured (Keating and Knight, 2007; Grunewald and Knight, 2011).

Brownstein and Tarr (1979) define three relaxation regimes for the fluid relaxing in a single pore: fast, intermediate and slow relaxation. In order to interpret the NMR data,

it is often assumed that the relaxation process in the most geologic applications of NMR occurs in the fast diffusion regime (Senturia and Robinson, 1970; Grunewald and Knight, 2009). In the absence of magnetic field inhomogeneities, three independent relaxation mechanisms for fluids in porous media contribute: surface relaxation time (T_{2S}), bulk fluid relaxation time (T_{2B}) and diffusion relaxation time (T_{2D}), which act in parallel. Therefore, the arithmetic mean of log T_2 (T_{2ml}) can be written as the harmonic sum of the distribution of relaxation times (Brownstein and Tarr, 1979):

$$\frac{1}{T_{2ml}} = \frac{1}{T_{2B}} + \frac{1}{T_{2S}} + \frac{1}{T_{2D}} \ , \tag{5}$$

where T_{2B}^{-1}, T_{2S}^{-1}, T_{2D}^{-1} are the average values for the entire pore space of the porous media.

The bulk relaxation time (T_{2B}) is the intrinsic relaxation property of a fluid that can be controlled by the physical properties of the fluid such as viscosity and chemical composition (Coates et al., 1999). Bulk relaxation time is measured by applying the CPMG pulse sequence on a sample of pore fluid placed in a large container. It is typically

considered that T_{2B} is considerably greater than T_{2S}, and so T_{2B}^{-1}<< T_{2S}^{-1}. Thus, it is often assumed that bulk fluid relaxation is negligible (Arns et al., 2005).

Surface relaxation occurs at the interface of fluid and grain, i.e., at the grain surface of the porous media, and follow as (Senturia and Robinson, 1970; Brownstein and Tarr, 1979; Godefroy et al., 2001):

$$\frac{1}{T_{2S}} = \rho_2 \frac{S}{V} = \rho_2 S_{por} , \quad (6)$$

where ρ_2 is the surface relaxivity of the pore walls (in ms^{-1}) and S_{por} is the volume-to-surface ratio of the pores (m^{-1}).

The diffusion relaxation time, T_{2D} is determined by (Carr and Purcell, 1954; Kleinberg and Horsfield, 1990; Fantazzini and Brown, 2005):

$$\frac{1}{T_{2D}} = \frac{D(\gamma G T_E)^2}{12} , \quad (7)$$

where D is diffusion coefficient of water ($D = 2.46 \times 10^{-9}\ {}^{m^2}/_{s}$; Simpson and Carr, 1958), γ is gyromagnetic gradient and T_E is the inter-echo spacing used in the CPMG sequence. The diffusion relaxation time is controlled by physical parameters such as viscosity and

temperature. By measuring the NMR response of a porous media at multiple echo times, the assumption that T_{2D} is negligible can be examined. If the variations of T_{2ml}^{-1} versus echo time are small then this assumption is valid (Kleinberg and Horsfield, 1990). If bulk and diffusion relaxation times are considered as negligible terms, equation 5 can be written as (Senturia and Robinson, 1970; Brownstein and Tarr, 1979; Godefroy et al., 2001):

$$\frac{1}{T_{2ml}} = \frac{1}{T_{2S}} = \rho_2 S_{por} = \rho_2 \alpha R^{-1} \ , \tag{8}$$

where R is the characteristic pore radius and α is a unitless geometric factor that depends on the shape of the pore ($\alpha = 1$ for planar pores, $\alpha = 2$ for cylindrical pores and $\alpha = 3$ for spherical pores).

PERMEABILITY ESTIMATION MODELS

Permeability estimation based on Induced Polarization (IP-k models)

SIP-permeability models are based on either relaxation time (τ) or quadrature conductivity (σ''). If quadrature conductivity (or phase) spectra have a distinct peak, models which are based on relaxation time can be used to predict the permeability (e.g.,

Revil et al., 2012) otherwise models based on quadrature conductivity (σ''), are often considered more appropriate to estimate permeability (e.g., Revil and Florsch, 2010; Weller et al., 2015) since a characteristic relaxation time cannot be determined. As illustrated in Figure 2, the phase spectra of investigated samples do not show a clearly defined peak. Therefore, we adopted the IP permeability models based on quadrature conductivity (σ''), Furthermore, since it is challenging to obtain a reliable IP data over a broad frequency range (mHz to kHz) in the field, a single frequency IP approach is likely to have more practical value. In what follows, the IP permeability models based on quadrature conductivity (σ'') measured at a frequency of 1 Hz is used.

The root mean square error ($RMSE$) of measured and modeled permeabilities can be used to assess the goodness of fit. Using log-transformed permeability, the RMSE is expressed as applied to the residual between the predicted permeability provided by different models and the measured permeability on a logarithmic scale:

$$\mathrm{RMSE} = \sqrt{\frac{1}{\mathrm{n}}\sum_{\mathrm{i}=1}^{\mathrm{n}}\left(\log \mathrm{k}_{\mathrm{predicted,i}} - \log \mathrm{k}_{\mathrm{measured,i}}\right)^2} \quad . \tag{9}$$

Revil and Florsch (2010) IP-permeability model

Development of permeability estimation models based on induced polarization (IP) is a result of a link between IP and surface area normalized to pore volume (S_{por}). IP models based on quadrature conductivity (σ'') are appropriate to estimate the permeability of materials without any distinct peak.

Revil and Cathles (1999) proposed a relationship between permeability (k), intrinsic formation factor (F), the mean grain size (d_0) and the cementation exponent (m) as:

$$k = \frac{{d_0}^2}{32m^2F(F-1)^2} \quad . \tag{10}$$

Revil and Florsch (2010) developed a mechanistic IP- k model based on equation 10. Their model defines permeability (k) as a function of F and σ'' by using the specific surface conductance of the Stern layer, Σ^S as follows:

$$\Sigma^S = \frac{\sigma'' d_0}{4}. \tag{11}$$

Substituting equation 11 into equation 10 yields:

$$k_{IP} = \frac{\Sigma^s}{2m^2F(F-1)^2}(\sigma'')^{-2}, \quad (12)$$

where σ'' is the quadrature conductivity (in S/m) at 1 Hz, m is the cementation factor (calculated from $F = \Phi^{-m}$), F is the measured intrinsic formation factor (unitless) and k_{IP} is predicted permeability (in m^2). This model is similar to the Börner et al. (1996) model, which is based on the Kozeny-Carman model.

Weller et al. (2015) IP permeability model

Weller et al. (2015) studied an extensive dataset of measurements on sandstone and unconsolidated sand materials. They compared different models for permeability estimation based on two parameters including formation factor and quadrature conductivity, which are related to porosity and the surface area normalized to pore volume, respectively. They considered empirical models (e.g., Rink and Schopper, 1974; Slater and Lesmes, 2002) and mechanistic models (e.g., Revil and Florsch, 2010; Revil,

2012). They proposed the following model for permeability prediction for sandstone samples:

$$k_{Sandstone} = \frac{2.66 \times 10^{-7}}{F^{5.35}\sigma''^{0.66}}, \quad (13)$$

and the following for unconsolidated sandy materials:

$$k_{Sand} = \frac{1.08 \times 10^{-13}}{F^{1.12}\sigma''^{2.27}}, \quad (14)$$

where $k_{sand/sandstone}$ is predicted permeability in m^2, F is the measured intrinsic formation factor (unitless) and σ'' is the quadrature conductivity (mS/m) at 1 Hz.

Permeability estimation based on Nuclear Magnetic Resonance (NMR-k models)

Kenyon et al. (1988) NMR permeability model

There are two kinds of NMR-K models: (1) Timur-Coates models, which are related to porosity determined from NMR measurements and the ratio of free fluid to bound fluid in the measured volume; (2) Schlumberger Doll Research (SDR) models which utilize porosity and NMR relaxation time (T_2) to estimate k (Seevers, 1966; Timur, 1969; Coates and Dumanoir, 1974). SDR models are often used to estimate the permeability of

reservoir samples. The SDR permeability model which utilizes the mean of log transverse relaxation time (T_{2ml}, it is given in Table 1) and porosity ϕ (Seevers, 1966; Kenyon et al., 1988; Straley et al., 1997; Kenyon, 1997):

$$k_{NMR} = bT_{2ml}{}^{c}\phi^{d}, \tag{15}$$

where T_{2ml} is in ms and k_{NMR} is predicted permeability in mD. b, c and d are empirically derived constants. The relaxation time exponent (*c*) is a result of dimensional analysis which considers the relationship between pore radius and relaxation time (Weller et al., 2014). However, the porosity exponent is a result of empirical studies (Coates et al., 1999; Dunn et al., 2002). Kenyon et al. (1988) proposed the following equation:

$$k_{NMR} = bT_{2ml}{}^{2}\phi^{4}. \tag{16}$$

The constant b in equation 16 is referred to as the lithologic constant, and is considered to fall within the range 4 to 5 mD/(ms)^2 from laboratory studies on sandstones (Morris et

al., 1996; Straley et al., 1997; Kenyon, 1997). The factor *b* for the sand samples tested was determined using measured and predicted permeability using equation 16 and minimizing the root mean square error (RMSE) defined as equation 9.

Permeability model derived from Johnson et al. (1986)

Johnson et al. (1986) reformulated the Katz and Thompson (1986) permeability model by introducing a parameter Λ (in m) as an effective surface area normalized to pore volume, or interconnected pore size and presented the following permeability model:

$$\mathrm{k} = \frac{\Lambda^2}{8\mathrm{F}} \cdot \tag{17}$$

The relationship between a length scale (grain radius or pore radius), SIP relaxation time and the diffusion coefficient of the counterions in the Stern layer of the electrical double layer ($\mathrm{D_S}$) can be expressed as:

$$\mathrm{l} = \sqrt{2\mathrm{D_s}\tau} \ , \tag{18}$$

where τ is the SIP relaxation time (in s) and the diffusion coefficient of the counterions in the stern layer $D_s = 1.29 \times 10^{-9}\ m^2 s^{-1}$for clean materials. Assuming that this length scale is equivalent to Λ in equation 17, then substituting equation 18 into equation 17 gives (Revil et al., 2012):

$$k = \frac{D_s \tau}{4F} \cdot \tag{19}$$

In a similar way, the length scale can also be considered related to the NMR relaxation time and the diffusion coefficient of the saturating fluid, D (Einstein, 1905; e.g. Keating and Falzone, 2013; Behroozmand et al., 2015):

$$l = \sqrt{6DT}\ , \tag{20}$$

where T is the arithmetic mean of log longitude or transverse relaxation time (T_{1ml} and T_{2ml} respectively). The diffusion coefficient of fluids in the porous media depends on the viscosity and temperature of the fluids. The samples analyzed here were saturated with 0.01M NaCl solution and the diffusion coefficient of sodium chloride solution is $1.619 \times 10^{-9}\ m^2 s^{-1}$ at 25°C (Guggenheim, 1954). If it is assumed the length scale in equation 20

is equivalent to Λ in equation 17, then substituting equation 20 into equation 17 gives (in terms of T_{2ml}):

$$k = \frac{3DT_{2ml}}{4F} \cdot \quad (21)$$

Induced Polarization-Nuclear Magnetic Resonance-Permeability Model (IP-NMR-k model)

Osterman et al. (2016) IP-NMR permeability model

Osterman et al. (2016) recently studied the permeability of sandstone samples using NMR and IP measurements. Their model is effectively an NMR-k model but utilizes IP measurements to determine a better estimate of the intrinsic formation factor, *F*, from an apparent formation factor observed at low salinities. They proposed a model based on the Johnson et al. (1986) reformulated Katz and Thompson (1986) permeability model (equation 17). The pore radius Λ can be determined from of the mean (or peak) NMR transverse relaxation time:

$$\Lambda = \rho_{2eff} T_{2p}, \quad (22)$$

where T_{2p} is the peak of NMR transverse relaxation time (in s), $\rho_{2eff} = \alpha a \rho_2$ is the effective surface relaxivity (in m/s) and *a* is 0.43 (see Osterman et al., 2016). Substituting equation 22 into equation 17 yields the following equation for permeability:

$$k = \frac{(\rho_{2eff} T_{2p})^2}{8F'}, \quad (23)$$

where F' is the IP-estimated intrinsic formation factor (equation 4).

RESULTS

Summary of properties

Table 1 shows the summary of physical properties obtained from all samples (sandstones and sands) along with measured IP and NMR parameters. The measured permeability of the samples spans over two orders of magnitude from 4.84×10^{-3} m^2 for sample 14-30H to 2.56×10^{-11} m^2 for sample 13-31H. The median grain size of the samples (d_{50}) varies between 106.3 μm (for sample 14-34H) to 409.6 μm (for sample 13-23H). Figure 2 shows example SIP and NMR responses of two samples: a sandstone (sample 15-10H) and a sand (sample 14-9H). Note that the SIP phase angle spectra do not show clearly defined peaks, indicating that a distinct dominant grain size is difficult to

resolve. Note also the low values of phase angles (and quadrature conductivity – spectra not shown) that are consistent with the clean (low clay content) nature of the samples. This was examined further by measuring the specific surface area (S_s) and the cation exchange capacity (CEC). The small values of specific surface area (S_s) (which results in the small values of surface area to volume ratio (S_{por})) and cation exchange capacity (CEC) for the samples is again consistent with a low clay content (see Table 1). The apparent formation factor, ($F_a = \sigma_f/\sigma'$ at 100mS/m) is noticeably smaller than the intrinsic formation factor, *F*, and for some cases unrealistically low (see Table 1). As can be seen in Table 1, the predicted formation factor using equation 4, F', is similar to apparent formation factor, F_a. That is, the correction factor proposed by Weller et al. (2013) does not appear to account well for the surface conductivity effect on the formation factor, for the samples analyzed here.

In order to assess the potential use of the IP-k models first the applicability of the modified Kozeny-Carman relationship i.e., the relationship between measured permeability and S_{por} ($k = \frac{a}{FS_{por}^b}$) is examined. Figure 3a shows a negative linear

relationship (as expected) between S_{por} and kF for measurements on the sand samples (pore surface area data were not collected for the sandstones).

In order to utilize the IP-k models which are based on linking the quadrature conductivity to surface area (e.g. Börner et al., 1996; Revil and Florsch, 2010) the link between IP and S_{por} is examined. As can be seen in Figure 3b, there is a significant positive relationship between σ'' and S_{por}, although it is noted that the quadrature conductivities of samples tested here are smaller than those shown in the relationship of Weller et al. (2010b), who reported a trend in the form of $\sigma'' = 1.03 \times 10^{-5} S_{por}^{0.992}$. Since Niu et al. (2016) observed that σ'' is correlated with S_{por}/F instead of S_{por}, the relationship between $\sigma'' F$ and S_{por} is tested (Figure 3c), although the correlation coefficient does not show improvement. With a significant positive relationship between quadrature conductivity (σ'') and S_{por}, a negative relationship between measured permeability and σ'', is expected, and confirmed in Figure 3d.

Revil and Florsch (2010) permeability model (IP-k model)

The Revil and Florsch (2010) model (equation 12) applied to measurements made on the sand and sandstone samples was examined. Figure 4 compares measured permeability with estimated permeability using this model. As can be seen from the Figure 4, there are some discrepancies between modeled and measured permeability values for some samples (particularly sand samples). The permeability model leads to a broader range of predicted permeability than that observed from the direct measurements of *k.*

Weller et al. (2015) permeability model (IP-k model)

The potential of the empirical models proposed by Weller et al. (2015) was tested. They proposed different models for sandstone and sandy materials (equations 13 and 14). They found that the formation factor is the most important term for prediction of sandstone permeability while the quadrature conductivity is significant in the estimation of permeability of sandy materials. As shown in Figure 5, the models show consistency in the overall trend but they tend to overestimate the permeability of the samples tested ($\mathrm{RMSE}_{\mathrm{Sandstone}} = 1.63$ and $\mathrm{RMSE}_{\mathrm{Sand}} = 2.45$).

***Kenyon et al. (1988)* permeability model (NMR-k model)**

In order to estimate the permeability from NMR relaxation measurements, the Kenyon et al. (1988) permeability model (equation 16) was examined on the sands and sandstones investigated in this study. The factor b in equation 16 was fitted to minimize the misfit in equation 9 and resulted in the value: 81.58 mD/(ms)^2 for sand samples. Following previous studies (discussed earlier) a value of 5 mD/(ms)^2 for a for the sandstone samples was adopted. Figure 6 shows that this model provides accurate permeability estimations for samples tested ($\mathrm{RMSE}_{\mathrm{Sandstone}} = 0.39$ and $\mathrm{RMSE}_{\mathrm{Sand}} = 0.69$) but the model is clearly calibrated for the sand samples.

The permeability model derived from *Johnson et al. (1986)*

The result from using the NMR model in equation 21 is shown in Figure 7a. The misfit between modeled and measured permeability, expressed as $RMSE,$ is 0.99 for sandstone and 0.64 for sand samples. This model appears applicable for the samples tested here and performance is significantly better than other models tested (IP or NMR). Given a principal aim here is to establish a relationship suitable for prediction of k in a practical setting and given that F may, in theory, be estimated using IP measurements

(as discussed earlier), it is useful to examine the performance of equation 21 with the intrinsic value of F replaced with that estimated value using IP (F'). The model's performance is still generally good ($RMSE =$ 1.06 for sandstone and 0.6 for sand), with estimates, on average, falling within one order of magnitude of measured k (Figure 7b). Clearly, for these samples, IP plays little role in correcting the apparent formation factor (as discussed above), however, adopting an IP correction may broaden the applicability to samples with higher clay content.

Osterman et al. (2016) model (IP-NMR-k model)

Osterman et al. (2016) derived relationships between (IP and NMR) geophysical parameters and the hydraulic parameters of the Katz and Thompson (1986) permeability model. Their model utilizes a predicted formation factor using IP parameters (real and quadrature conductivity measured at 1 Hz) through equation 4. Figure 8 shows some significant deviation between the formation factor estimated from σ' and σ'' using a single salinity measurement (equation 4) and the intrinsic formation factor obtained from multi-salinity measurements. In fact, because of the low quadrature conductivities observed in the investigated samples here, the correction term in equation 4 has limited effect.

Despite these discrepancies in estimated formation factor, the model of Osterman et al. (2016) (equation 23) is examined. As can be seen in Figure 9, this model generally underestimates the permeability of the sandstone and sand samples ($RMSE_{\text{Sandstone}} = 1.81$ and $\text{RMSE}_{\text{Sand}} = 1.95$).

The discrepancies between measured and modeled permeability using the Osterman et al. (2016) model may be partially due to errors in the calculated formation factor (F'). However, as the values of F' tend to underestimate the true formation factor its effect will be an overestimation of permeability.

DISCUSSION

The main aim of this study is to test the applicability of different permeability models that incorporate IP and NMR parameters to predict the permeability of hydrocarbon reservoir samples. In order to evaluate the quality of the fit between measured and predicted permeability the root mean square error between predicted and measured permeability and average deviation (d) are calculated:

$$\mathrm{d} = \frac{1}{\mathrm{n}} \sum_{\mathrm{i}=1}^{\mathrm{n}} |\log \mathrm{k}_{\mathrm{predicted,i}} - \log \mathrm{k}_{\mathrm{measured,i}}|, \quad (24)$$

where n is the number of sample tested ($\mathrm{n} = 8$ for sandstone and $\mathrm{n} = 22$ for sand), $\mathrm{k}_{\mathrm{predicted}}$ is the estimated permeability of samples using current permeability equations and $\mathrm{k}_{\mathrm{measured}}$ is the measured value of permeability of samples. Table 2 summarizes the results.

These statistics (RMSE and d) provide a quantitative evaluation of the predictive quality for different models. A value of $\mathrm{d} = 1$ indicates an average deviation of one order of magnitude. The lowest value of RMSE and d for the sandstones tested is from the Kenyon et al. (1988) model ($\mathrm{RMSE} = 0.39$ and $\mathrm{d} = 0.34$), but it is noted that the factor *a* in the model, for the sands samples, was calibrated to minimize the RMSE and thus it is not surprising that this model performs best. The model based on Johnson et al. (1986) (equation 21) gives the lowest value of RMSE and *d* for sand ($\mathrm{RMSE} = 0.57$ and $\mathrm{d} = 0.51$). Application of this model also reveals a significant correlation between measured and predicted permeabilities ($R^2_{Sandstone} = 0.49$ and $R^2_{Sand} = 0.68$). The estimation of the permeability of samples investigated here using the Revil and Florsch (2010) model

provides a low value for d, but a weak correlation coefficient between measured and predicted permeabilities of sand samples ($R^2_{Sand} = 0.02$). The empirical model of Weller et al. (2015) and Osterman et al. (2016) result in the highest root mean square error and average deviation and so the lowest predictive quality for sand and sandstone sample types, respectively. As noted earlier, the Weller et al. (2015) model overestimates the permeability of samples tested here (see Figure 5); however, the Osterman et al. (2016) model underestimates the permeability of samples investigated in this study. It may be that their empirical models are more applicable to clayey sands and sandstones.

From the comparison between IP-k models (Figures 4 and 5) and the NMR-k model (Figure 6) it is seen that the NMR-k model predicts the permeability of investigated samples better, but the factor *a* needs to be derived from a calibration process (for the sand samples) and thus the comparison of performances is somewhat biased. The Osterman et al. (2016) model uses the NMR parameter ($\mathrm{T_{2p}}$) and IP parameters (formation factor based on real and imaginary conductivity, σ' and σ'') to estimate the permeability. As observed in Figure 9, the performance of the Osterman et al. (2016)

model for sandstone and sand samples is poor and errors vary over one order of magnitude (this model underestimates the permeability of samples), however a significant relationship between the measured and estimated permeabilities is observed ($R^2_{Sandstone} = 0.57$ and $R^2_{Sand} = 0.68$). The derived model based on Johnson et al. (1986) (assuming a relationship between length scale and NMR relaxation time) gives an improved model that appears applicable for tested sand and sandstone samples. The model was examined with the calculated formation factor (F'): this model appears applicable, in particular for the sand samples. In order to evaluate of the validity of the derived model (equation 21), further tests are needed on a wider dataset of measurements on clean and clayey sands and sandstones.

Given the low surface conductivity of the samples tested here it is useful to examine the tested models with a simpler approach based on real conductivity (σ') , e.g., a property directly obtainable from DC resistivity surveys. To do this we used the empirical model proposed by Purvance and Andricevic (2000):

$$k = a(\sigma')^b \ , \qquad (25)$$

where a and b are calibration parameters, which we evaluated separately for the two sample types. As can be seen in Figure 10, this model provides a reliable permeability prediction for the samples tested but requires calibration of model parameters for samples. Therefore, the values of a and b may vary for different datasets. It would appear that if calibration is necessary for NMR-k or SIP-k models (e.g. the Kenyon et al., 1988 model) then, for these samples, a simpler approach based on real conductivity may be more effective. However, results from the application of a model based on Johnson et al. (1986) utilizing NMR data in an uncalibrated fashion show greater promise.

For the samples tests, and the models compared, NMR measurements appears to offer greater value in estimating permeability. The IP-based models predict a range of permeability that is broader than the two orders of magnitude measured on the samples. Furthermore, attempts to correct the apparent formation factor demonstrated little, if any, additional information in the IP measurements. Many previous IP models for permeability estimation have, understandably, investigated samples with a wide range of permeabilities, however, when focusing on a narrow range (as here) the resolution

limitations of such models may be revealed. Under such cases site specific calibrations, i.e. local empirical models, may be the most effective means of utilizing geophysical data for permeability estimation.

CONCLUSIONS

Many different models have been developed to estimate the permeability, k, of rocks and soils using IP and NMR measurements. A set of IP and NMR measurements on 22 sand and eight sandstone samples were used to evaluate the applicability of different IP, NMR and IP-NMR models to predict the permeability. Two IP-k models, based on the quadrature conductivity, show reasonable capacity to predict the trend in observed permeability but accurate estimation of permeability for a given sample is weak. In contrast, an established NMR-k model that is based on porosity (ϕ) and the arithmetic mean of log transverse relaxation time (T_{2ml}) provides a better permeability prediction for the samples but requires calibration of a model coefficient for sand samples. Application of a recently proposed IP-NMR-k model reveals consistent underestimation of the permeability of the sandstone and sand samples tested.

Building on earlier studies, a new NMR-k model was derived. This model predicts well the permeability of samples tested here. Substituting the intrinsic formation factor with a single salinity estimate enhanced by IP measurements to account for surface conductivity, provides a reasonable permeability prediction for sand samples but leads to some deterioration in performance of the permeability model for the sandstone samples. However, the overall performance from these initial tests appears good and worthy of further testing. In order to validate and generalize this model, there is a need to test it on data sets from samples of different lithologies including clayey sands and sandstones.

Geophysical estimation of permeability remains a key challenge in hydrogeophysics. Several models have been proposed and new ones develop. Through continued appraisal of these models with new datasets, such as those described here, may lead to reliable and robust techniques that can exploit the potential of geophysical measurements for improved in-situ permeability characterization. Although some models may appear to perform relatively poorly, being able to estimate permeability within one order of magnitude through geophysical measurements is often likely to be extremely

valuable. The key challenge is ensuring universal applicability of models, for reliable estimation. Such a challenge can only be addressed through model testing, as done here.

ACKNOWLEDGMENTS

We thank Iranian Offshore Oil Company (IOOC) for providing the plug samples for this research. We also thank Gordon Osterman and Kristina Keating (Rutgers University) for assistance with the NMR data interpretation and Serge Galaup and Lea' Pigot (EA4592 – Bordeaux INP- UBM, France) for assistance with the BET data acquisition. David Lewis (Lancaster University) fabricated the SIP sample holders – his support for this work is appreciated. We appreciate the comments from the Associate Editor and four reviewers.

REFERENCES

Archie, G. E., 1942, The electrical resistivity log as an aid in determining some reservoir characteristics: Transactions of the American Institute of Mining and Metallurgical Engineers., **146**, no. 1, 54–62, doi:10.11159/ijmem.2012.008.

Arns, C., M. Knackstedt, and N. Martys, 2005, Cross-property correlations and permeability estimation in sandstone: Physical Review E, **72**, no. 4, 1–12, doi:10.1103/PhysRevE.72.046304.

Allen, D., C. Flaum, T. Ramakrishnan, J. Bedford, K. Castelijns, D. Fairhurst, G. Gubelin, N. Heaton, C. C. Minh, M. A. Norville, M. R. Seim, T. Pritchard, and R. Ramamoorthy, 2000: Trends in NMR logging: Oilfield Review/Schlumberger, **12**, no. 2, 2–19.

Banavar, J. R., and L. M. Schwartz, 1987, Magnetic resonance as a probe of permeability in porous media: Physical Review Letters, **58**, no. 14, 1411–1414.

Behroozmand, A., K. Keating, and E. Auken, 2015, Review of the Principles and Applications of the NMR Technique for Near-Surface Characterization: Surveys in Geophysics, **36**, no. 1, 27–85, doi: 10.1007/s10712-014-9304-0.

Binley, A., L. Slater, M. Fukes, and G. Cassiani, 2005, Relationship between spectral induced polarization and hydraulic properties of saturated and unsaturated sandstone: Water Resources Research, **41**, no. 12, W12417.

Bloch, F., 1946, Nuclear induction: Physical Review, **70**, no. 7-8, 460–474.

Börner, F. D., J. R. Schopper, and A. Weller, 1996, Evaluation of transport and storage properties in the soil and groundwater zone from induced polarization measurements: Geophysical Prospecting, **44**, no. 4, 583–601.

Bryar, T. R., C. J. Daughney, R. J. Knight, 2000, Paramagnetic effects of iron (III) species on nuclear magnetic relaxation of fluid protons in porous media: Journal of Magnetic Resonance, **142**, no. 1, 74–85.

Brownstein, K. R., and C. E. Tarr, 1979, Importance of classical diffusion in NMR studies of water in biological cells: Physical Review A, **19**, no. 6, 2446–2453.

Brunauer, S., P. H. Emmett, and E. Teller, 1938, Adsorption of gases in multimolecular layers: Journal of the American Chemical Society, **60**, no. 2, 309–319.

Carr, H. Y., and E. M. Purcell, 1954, Effects of diffusion on free precession in nuclear magnetic resonance experiments: Physical Review, **94,** no. 3, 630–638.

Coates, G. R., and I. L. Dumanoir, 1974, New approach to improved log-derived permeability: The Log Analyst, **15**, no. 1, 17–31.

Coates, G. R., H. J. Vinegar, P. N. Tutunjian, and J. S. Gardner, 1993, Restrictive diffusion from uniform gradient NMR well logging: Presented at the 68th Annual Technical Conference and Exhibition of the Society of Petroleum Engineers, Paper SPE 26472.

Coates, G. R., L. Xiao, and G. Prammer, 1999, NMR logging principles and applications: Haliburton Energy Services, Houston.

Cohen, M. H., and K. S. Mendelson, 1982, Nuclear magnetic relaxation and the internal geometry of sedimentary rocks: Applied Physics, **53**, no. 2, 1127–1135, doi:10.1063/1.330526.

Dakhnov, V. N., M. G. Latishova, and V. A. Ryapolov, 1967, Well logging by means of induced polarization (electrolytic logging): The Log Analyst, **8**, no. 3, 3-18.

de Lima, O. A. L., and S. Niwas, 2000, Estimation of hydraulic parameters of shaly sandstone aquifers from geoelectrical measurements: Hydrology, **235**, no. 1-2, 12–26, doi:10.1016/S0022-1694(00)00256-0.

Dunn, K. J., D. J. Bergman, and G. A. LaTorraca, 2002, Nuclear magnetic resonance-Petrophysical and logging application: Handbook of Geophysical Exploration, Seismic Exploration, **32**, Pergamon Press.

Einstein, A., 1905, Über die von der molekularkinetischen Theorie der Wärme geforderte Bewegung von in ruhenden Flüssigkeiten suspendierten Teilchen: Annalen der Physik, **322**, no. 8, 549-560.

Fantazzini, P., and R. J. S. Brown, 2005, Initially linear echo-spacing dependence of 1/T2 measurements in many porous media with pore-scale inhomogeneous fields: Journal of Magnetic Resonance, **177**, no. 2, 228–235.

Foley, I., S. A. Farooqui, and R. L. Kleinberg, 1996, Effect of paramagnetic ions on NMR relaxation of fluids at solid surfaces: Journal of Magnetic Resonance, Series A, **123**, no. 1, 95–104.

Godefroy, S., J. P. Korb, M. Fleury, and R. G. Bryant, 2001, Surface nuclear magnetic relaxation and dynamics of water and oil in macroporous media: Physical Review E, Statistical, nonlinear, and soft matter physics, **64**, no. 2, 216051–2160513.

Guggenheim, E. A., 1954, The diffusion coefficient of sodium chloride: Transactions of Faraday Society, **50**, no. 10, 1048-1051.

Grunewald, E., and R. Knight, 2009, A laboratory study of NMR relaxation times and pore coupling in heterogeneous sediment: Geophysics, **74**, no. 6, E215–E221.

Grunewald, E., and R. Knight, 2011, A laboratory study of NMR relaxation times in heterogeneous media: Geophysics, **76**, no. 4, G73–G83.

Hertrich, M., 2008, Imaging of groundwater with nuclear magnetic resonance: Progress in Nuclear Magnetic Resonance Spectroscopy, **53**, no. 4, 227–248.

Johnson, D., J. Koplik, and L. Schwartz, 1986, New pore-size parameter characterizing transport in porous media: Physical Review Letters, **57**, no. 20, 2564–2567, doi:10.1103/PhysRevLett.57.2564.

Katz, A., and A. Thompson, 1986, Quantitative prediction of permeability in porous rock: Physical Review B, **34**, no. 11, 8179–8181, doi:10.1103/ PhysRevB.34.8179.

Keating, K., and S. Falzone, 2013, Relating nuclear magnetic resonance relaxation time distributions to void-size distributions for unconsolidated sand packs: Geophysics, **78**, no. 6, D461–D472.

Keating, K., and R. Knight, 2007, A laboratory study to determine the effect of iron oxides on proton NMR measurements: Geophysics **72**, no. 1, E27–E32.

Keating, K., and R. Knight, 2010, A laboratory study of the effect of Fe (II)-bearing minerals on nuclear magnetic resonance (NMR) relaxation measurements: Geophysics, **75**, no. 3, F71–F82.

Keating, K., and R. Knight, 2012, The effect of spatial variation in surface relaxivity on nuclear magnetic resonance relaxation rates: Geophysics, **77**, E365–E377.

Kenyon, W. E., P. I. Day, C. Straley, and J. F. Willemsen, 1988, A three-part study of NMR longitudinal relaxation properties of water saturated sandstones: Society of Petroleum Engineers Formation Evaluation, **3**, no. 3, 622–636.

Kenyon, W. E., 1997, Petrophysical principles of applications of NMR logging: The Log Analyst, **38**, no. 2, 21–43.

Kemna, A., H. M. Münch, K. Titov, E. Zimmermann, and H. Vereecken, 2005, Relation of SIP relaxation time of sands to salinity, grain size and hydraulic conductivity: in Proceedings of the 11th European Meeting of Environmental and Engineering Geophysics, Extended Abstracts: Near Surface 2005, P054.

Kleinberg, R., and M. Horsfield, 1990, Transverse relaxation processes in porous sedimentary rock: Magnetic Resonance, **88**, no. 1, 9–19, doi: 10.1016/0022-2364(90)90104-H.

Kleinberg, R. L., W. E. Kenyon, and P. P. Mitra, 1994, Mechanism of NMR relaxation of fluids in rock: Magnetic Resonance, **108**, no. 2, 206–214.

Legchenko, A., J. M. Baltassat, A. Beauce, and J. Bernard, 2002, Nuclear magnetic resonance as a geophysical tool for hydrogeologists: Applied Geophysics, **50**, no. 1, 21–46.

Lesmes, D. P., and S. P. Friedman, 2005, Relationships between the electrical and hydrogeological properties of rocks and soils. In: Rubin, Y. and Hubbard S.S. (Eds.) Hydrogeophysics. Springer, The Netherland, 87-128.

Meju, M. A., P. Denton, and P. Fenning, 2002, Surface NMR sounding and inversion to detect groundwater in key aquifers in England: comparisons with VES-TEM methods: Applied Geophysics, **50**, no. 1-2, 95–111.

Morris, C. E., P. Deusch, R. Freedman, D. Mckeon, and R. L. Kleinberg, 1996, Operating guide for the combinable magnetic resonance tool: The Log Analyst, **37**, no. 6, 53–60.

Osterman, G., K. Keating, A. Binley, and L. Slater, 2016, A laboratory study to estimate pore geometric parameters of sandstones using complex conductivity and nuclear magnetic resonance for permeability prediction: Water Resources Research, **52**, no. 6, 4321–4337, doi:10.1002/2015WR018472.

Purvance, D. T., and R. Andricevic, 2000, On the electrical-hydraulic conductivity correlation in aquifers: Water Resources Research, **36**, no. 10, 2905–2913.

Revil, A., 2012, Induced polarization of shaly sands: Influence of the electrical double layer: Water Resources Research, 48, W02517.

Revil, A., A. Binley, L. Mejus, and P. Kessouri, 2015, Predicting permeability from the characteristic relaxation time and intrinsic formation factor of complex conductivity

spectra: Water Resources Research, **51**, no. 8, 6672–6700, doi:10.1002/2015WR017074

Revil, A., K. Koch, and K. Holliger, 2012, Is it the grain size or the characteristic pore size that controls the induced polarization relaxation time of clean sands and sandstones?: Water Resources Research, **48**, no. 5, W05602, doi:10.1029/2011WR011561.

Revil, A., and L. M. Cathles, 1999, Permeability of shaly sands: Water Resources Research, **35**, no. 3, 651–662.

Revil, A., and N. Florsch, 2010, Determination of permeability from spectral induced polarization in granular media: Geophysics, **181**, no. 3, 1480–1498.

.

Seevers, D. O., 1966, A nuclear magnetic method for determining the permeability of sandstones: 33rd annual logging symposium, society of professional well log analysts, transactions, paper L.

Senturia, S. D., and J. D. Robinson, 1970, Nuclear spin-lattice relaxation of liquids confined in porous solids: Society of Petroleum Engineers, **10**, no. 3, 237–244.

Simpson, J. H., and H. Y. Carr, 1958, Diffusion and nuclear spin relaxation in water: Physical Review, **111**, no. 5, 1201–1202.

Slater, L., 2007, Near surface electrical characterization of hydraulic conductivity: From petrophysical properties to aquifer geometries — A review: Surveys in Geophysics, **28**, no. 2, 169–197.

Slater, L., and D. P. Lesmes, 2002, Electrical-hydraulic relationships observed for unconsolidated sediments: Water Resources Research, 38, 1213, doi: 10.1029/2001WR001075.

Straley, C., D. Rossini, H. Vinegar, P. Tutunjian, and C. Morriss, 1997, Core analysis by low-field NMR: The Log Analyst, **38**, no. 2, 84–93.

Sturrock, J. T., D. Lesmes, and F. D. Morgan, 1998, The influence of micro-geometry on the hydraulic permeability and the induced polarization response of sandstones,

In: Proceedings of the Symposium on the Application of Geophysics to Engineering and Environmental Problems (SAGEEP), 859–867.

Sturrock, J. T., 1999, Predictions of hydraulic conductivity using spectral induced polarizations: MS dissertation. Boston College.

Timur, A., 1969, Producible porosity and permeability of sandstones investigated through nuclear magnetic resonance principle: The Log Analyst, **10**, no. 1, 3-11.

Torrey, H. C., 1956, Bloch equations with diffusion terms: Physical Review, **104**, no. 3, 563–565.

Vinegar, H. J., and M. Waxman, 1984, Induced polarization of shaly sand: Geophysics, **49**, no. 8, 1267–1287, doi:10.1190/1.1441755.

Vogeley, J. R., and C. O. Moses, 1992, H NMR relaxation and rock permeability: Geochimica et Cosmochimica Acta, **56**, no. 7, 2947–2953.

Weller, A., S. Nordsiek, and W. Debschütz, 2010a, Estimating permeability of sandstone samples by nuclear magnetic resonance and spectral-induced polarization: Geophysics **75**, no. 6, E215–E226.

Weller, A., L. Slater, S. Nordsiek, and D. Ntarlagiannis, 2010b, On the estimation of specific surface per unit pore volume from induced polarization: A robust empirical relation fits multiple data sets: Geophysics, **75**, no. 4, WA105–WA112, doi: 10.1190/1.3471577.

Weller, A., L. Slater, and S. Nordsiek, 2013, On the relationship between induced polarization and surface conductivity: Implications for petrophysical interpretation of electrical measurements: Geophysics, **78**, no. 5, D315–D325, doi:10.1190/geo2013-0076.

Weller, A., M. Kassab, W. Debschütz, and C. Sattler, 2014, Permeability prediction of four Egyptian sandstone formations: Arabian Journal of Geoscience, **7**, no. 12, 5171–5183, doi: 10.1007/s12517-013-1188-7

Weller, A., L. Slater, A. Binley, S. Nordsiek, and S. Xu, 2015, Permeability prediction based on induced polarization: Insights from measurements on sandstone and unconsolidated samples spanning a wide permeability range: Geophysics, **80**, no. 2, D161–D173, doi:10.1190/ GEO2014-0368.1.

Worthington, P. F., and F. A. Collar, 1984, Relevance of induced polarization to quantitative formation evaluation: Marine and Petroleum Geology, **1**, no. 1, 14-26.

Yaramanci, U., G. Lange, and K. Knödel, 1999, Surface NMR within a geophysical study of an aquifer at Haldensleben (Germany): Geophysical Prospecting, **47**, no. 6, 923–943.

Yaramanci, U., G. Lange, and M. Hertrich, 2002, Aquifer characterisation using surface NMR jointly with other geophysical techniques at the Nauen/Berlin test site: Applied Geophysics, **50**, no. 1-2, 47–65.

Zimmermann, E., A. Kemna, J. Berwix, W. Glaas, and H. Vereecken, 2008, EIT measurement system with high phase accuracy for the imaging of spectral induced

polarization properties of soils and sediments: Measurement Science and Technology, **19**, no. 9, 094010, doi:10.1088/0957-0233/19/9/ 094010.

Zisser, N., A. Kemna, and G. Nover, 2010, Relationship between low-frequency electrical properties and hydraulic permeability of low permeability sandstones: Geophysics, **75**, no. 3, E131–E141, doi:10.1190/1.3413260.

LIST OF FIGURES

Figure 5. IP Modeled permeability versus measured permeability based on the Weller et al. (2015) models. $R^2_{Sandstone} = 0.36$ and $R^2_{Sand} = 0.46$.

Figure 6. NMR predicted permeability versus measured permeability based on the Kenyon et al. (1988) model. $R^2_{Sandstone} = 0.58$ and $R^2_{Sand} = 0.73$.

Figure 7. Predicted permeability versus measured permeability using equation 21. (a) using the intrinsic formation factor, F, calculated from multi-salinity measurements ($R^2_{Sandstone} = 0.49$ and $R^2_{Sand} = 0.68$) (b) using the formation factor, F', estimated from equation 4 ($R^2_{Sandstone} = 0.53$ and $R^2_{Sand} = 0.55$).

Figure 8. The relationship between intrinsic formation factor calculated from multi-salinity measurements (F) and calculated formation factor from equation 4 (F').

Figure 9. The relationship between measured and predicted permeability using the Osterman et al. (2016) model. $R^2_{Sandstone} = 0.57$ and $R^2_{Sand} = 0.68$.

Figure 10. The relationship between measured and predicted permeability using the resistivity model proposed by Purvance and Andricevic (2000).

LIST OF TABLES

Table 1. Summary of physical properties and measured IP and NMR parameters of sandstone and sand samples.

Parameter	Min	Max	Mean
Porosity, ϕ (%)	27.65	41.00	34.69
Intrinsic formation factor, F (from multi-salinity measurements)	2.74	9.84	4.62
Apparent formation factor, F_a (measured at 100mS/m)	1.43	7.22	4.1
Predicted formation factor, F' (using equation 4)	1.44	7.31	4.16
Surface area-to-volume ratio, S_{por} (μm^{-1})	0.46	11.78	2.04
Permeability, k (m^2)	4.84×10^{-13}	2.56×10^{-11}	1.01×10^{-11}
Median grain diameter, d_{50} (μm)	106.27	409.57	242.51
Cation exchange capacity (meq/100g)	0.19	1.79	0.50
Quadrature conductivity, σ'' (S/m)	2.16×10^{-6}	1.16×10^{-4}	1.50×10^{-5}
NMR transverse relaxation time, T_2 (s)	0.0093	0.74	0.25

Table 2. The root mean square error (RMSE) and average deviation (*d*) between measured and predicted permeability for different models. RMSE is defined in equation (9) and *d* is defined in equation 24. Both *RMSE* and *d* are based on the logarithm of permeability in units of m^2.

Permeability Model	**$RMSE_{Sandstone}$**	**$RMSE_{Sand}$**	**$d_{Sandstone}$**	**d_{Sand}**
Revil and Florsch (2010) IP-k model (equation 12)	0.54	1.05	0.42	0.84
Weller et al. (2015) model (equation 13 and 14)	1.63	2.45	1.58	2.38
Kenyon et al. (1988) NMR-k model, a=5 (equation 16)	0.39	-	0.34	-
Kenyon et al. (1988) NMR-k model, a=88.43 (equation 16)	-	0.69	-	0.55
NMR model derived from Johnson et al. (1986) model (equation 21)	0.99	0.57	0.96	0.51
IP-NMR model derived from Johnson et al. (1986) model (equation 21 with F')	1.06	0.60	1.04	0.55
Osterman et al. (2016) IP_NMR-k model (equation 23)	1.81	1.95	1.73	1.67

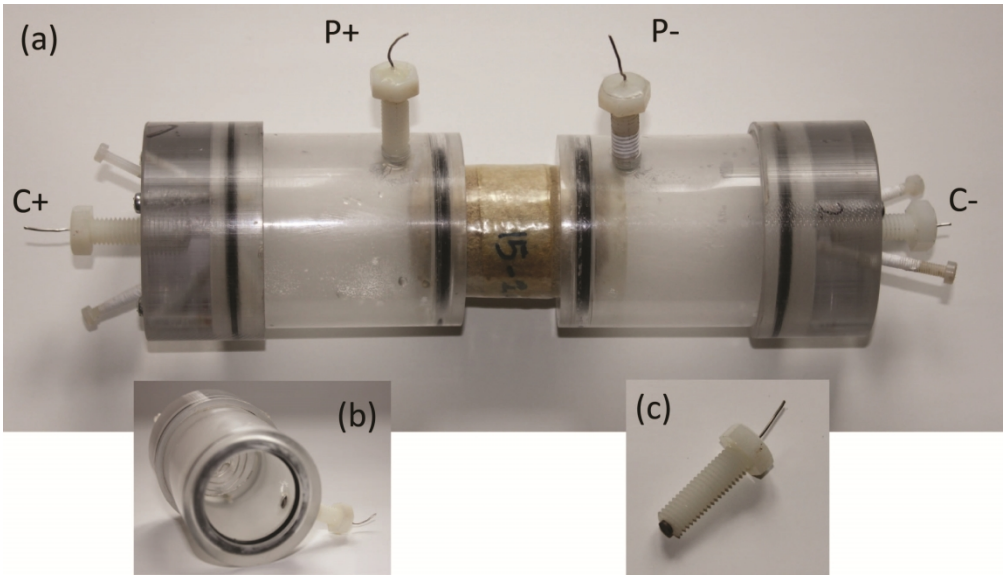

Figure 1. (a) Sample holder arrangement for SIP measurements on sandstone and sand samples, (b) current electrode (Ag coil) and (c) potential electrode (Ag-AgCl).

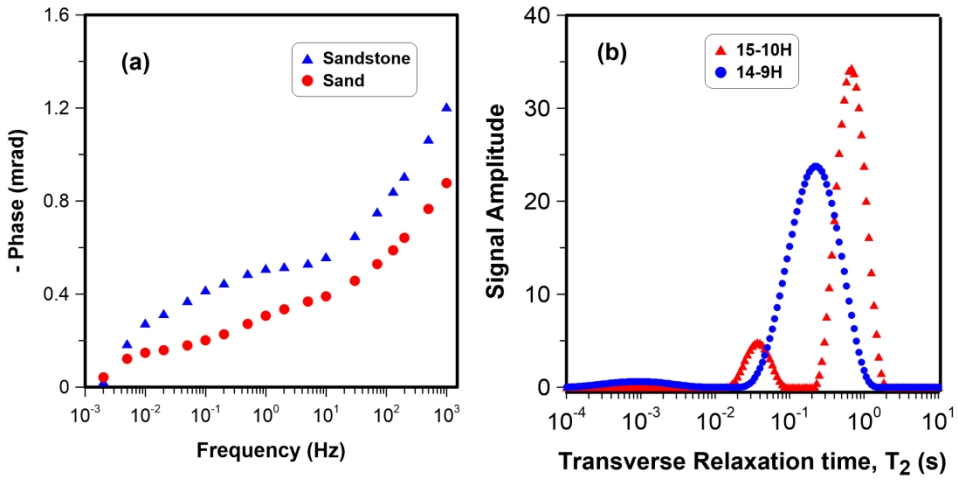

Figure 2. (a) Example SIP response of two samples (sandstone sample 15-10H and sand sample 14-9H). (b) Example NMR response of two samples (sandstone sample 15-10H and sand sample 14-9H).

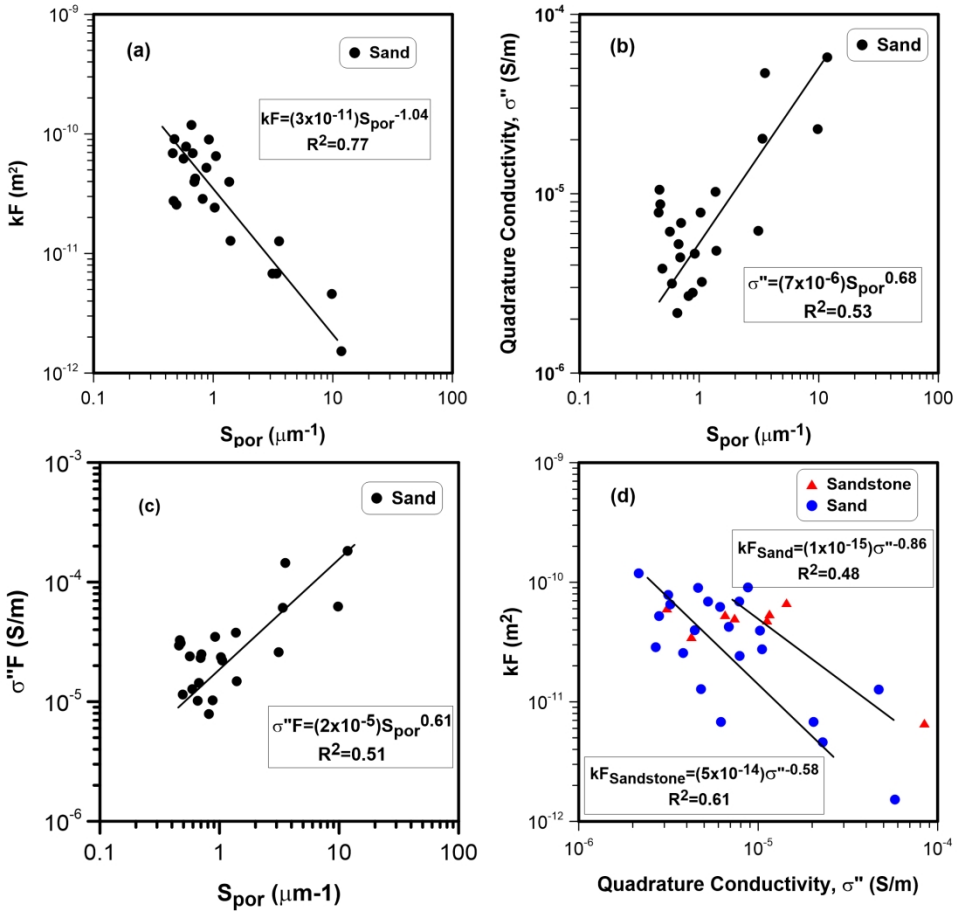

Figure 3. (a) The relationship between the product of measured permeability and the formation factor (kF) and S_por. (b) The relationship between quadrature conductivity (σ") and S_por. (c) The relationship between the product of quadrature conductivity and the formation factor (σ^" F) and S_por. (d) The relationship between the product of measured permeability and the formation factor (kF) and quadrature conductivity (σ").

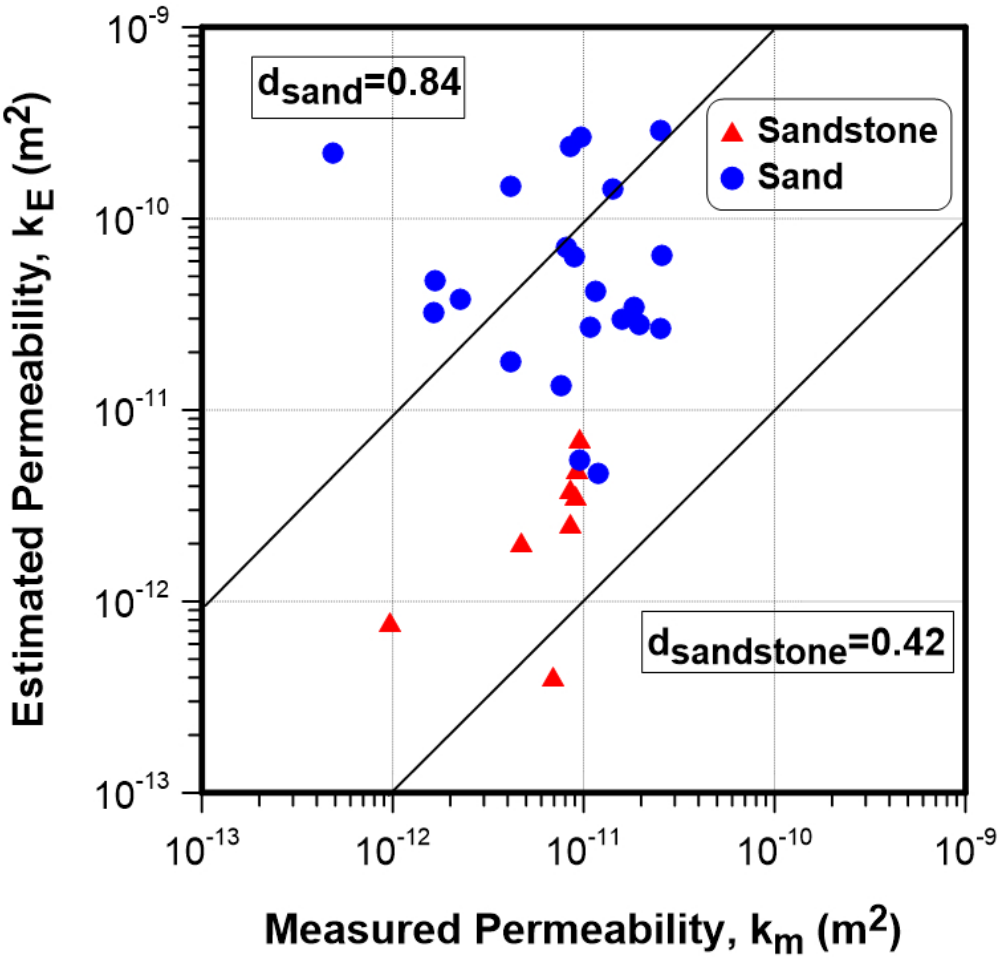

Figure 4. IP modeled permeability versus measured permeability based on the Revil and Florsch (2010) model. R_Sandstone^2=0.33 and R_Sand^2=0.02.

199x191mm (96 x 96 DPI)

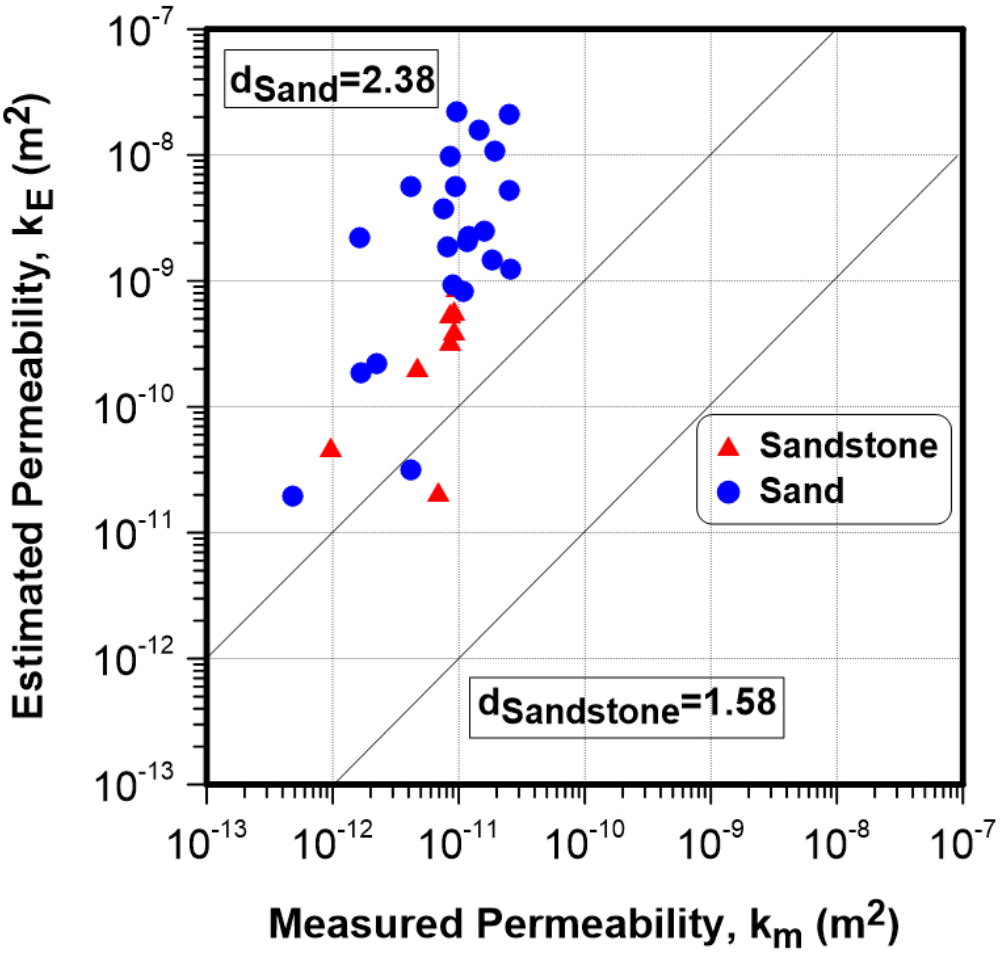

Figure 5. IP modeled permeability versus measured permeability based on the Weller et al. (2015) models. R_Sandstone^2=0.36 and R_Sand^2=0.46.

201x192mm (96 x 96 DPI)

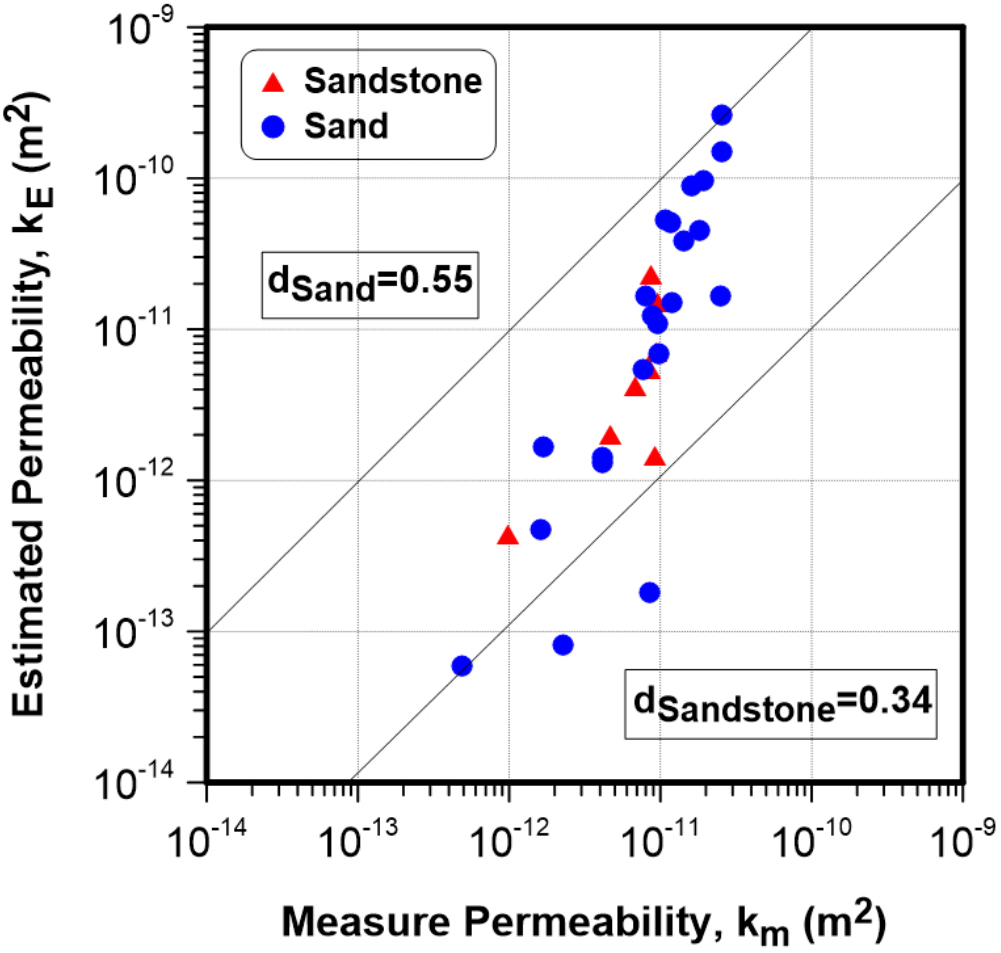

Figure 6. NMR predicted permeability versus measured permeability based on the Kenyon et al. (1988) model. R_Sandstone^2=0.58 and R_Sand^2=0.73.

201x192mm (96 x 96 DPI)

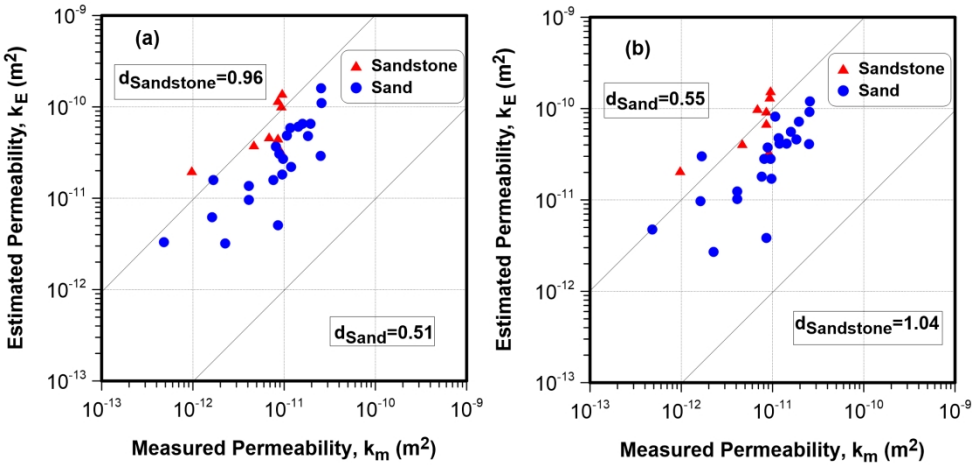

Figure 7. Predicted permeability versus measured permeability using equation 21. (a) using the intrinsic formation factor, F, calculated from multi-salinity measurements (R_Sandstone^2=0.49 and R_Sand^2=0.68). (b) using the formation factor, F', estimated from equation 4 (R_Sandstone^2=0.53 and R_Sand^2=0.55).

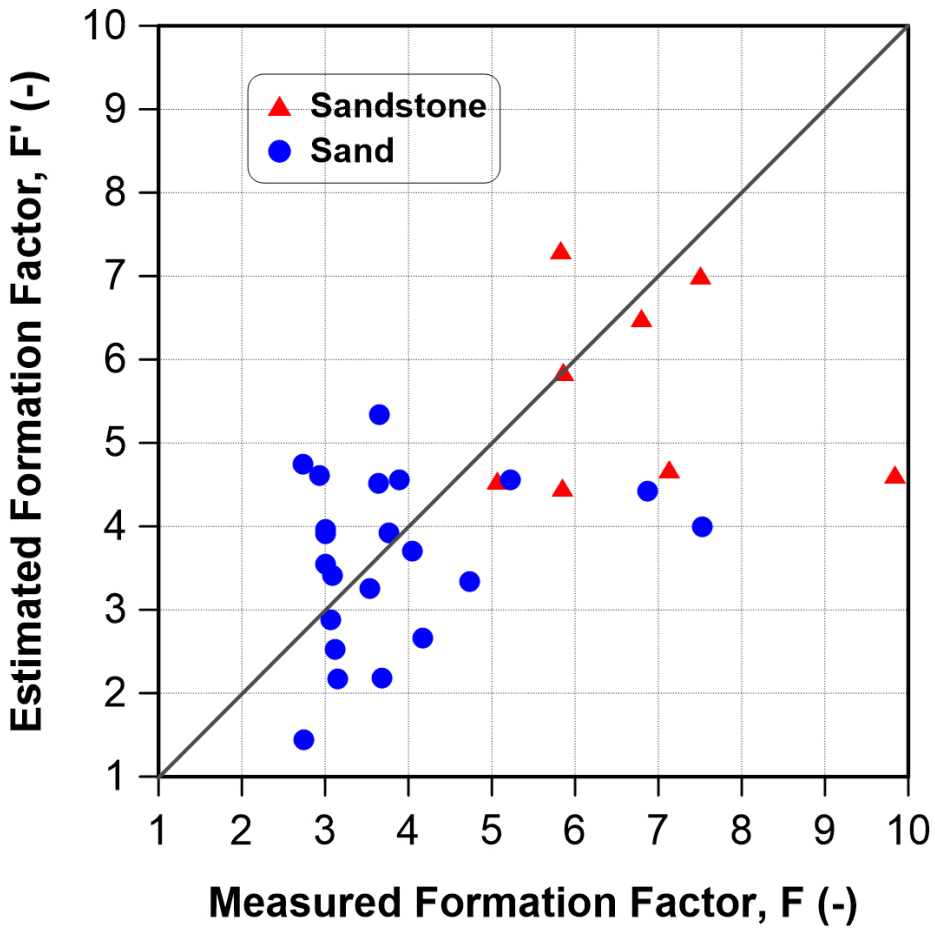

Figure 8. The relationship between intrinsic formation factor calculated from multi-salinity measurements (F) and calculated formation factor from equation 4 (F').

203x187mm (144 x 144 DPI)

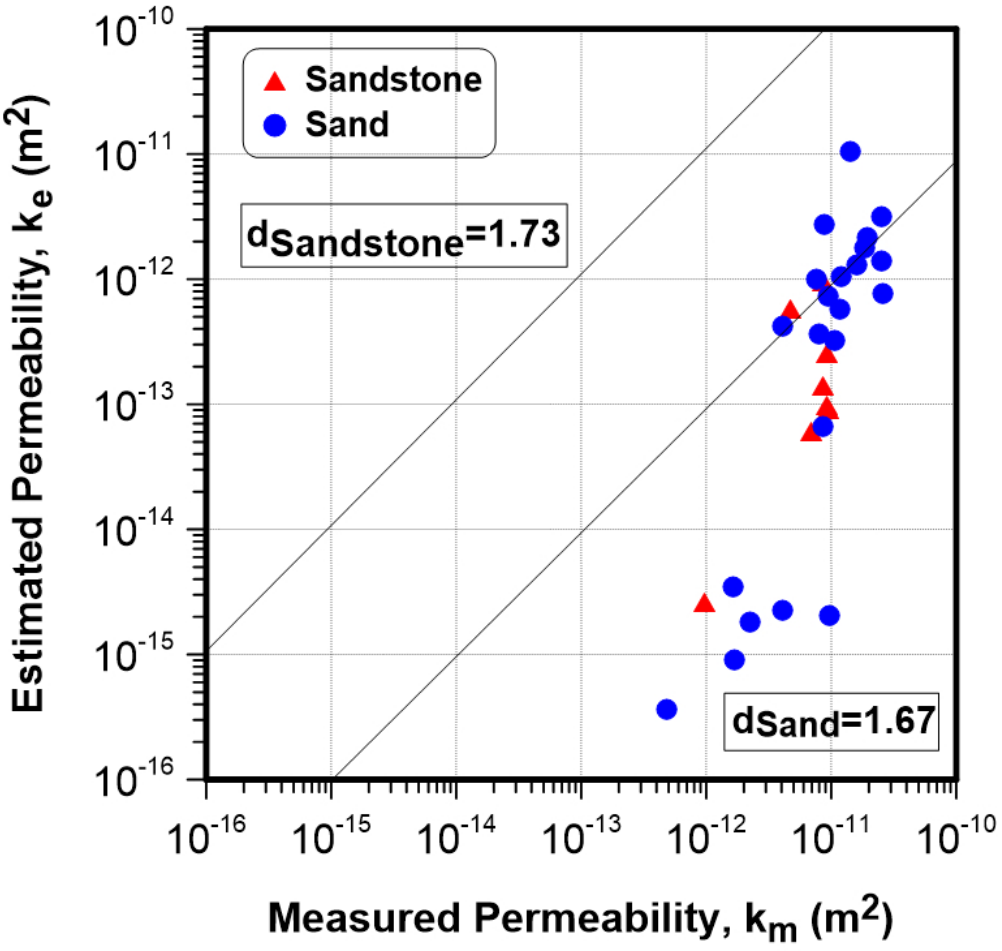

Figure 9. The relationship between measured and predicted permeability using the Osterman et al. (2016) model. R_Sandstone^2=0.57 and R_Sand^2=0.68.

203x192mm (96 x 96 DPI)

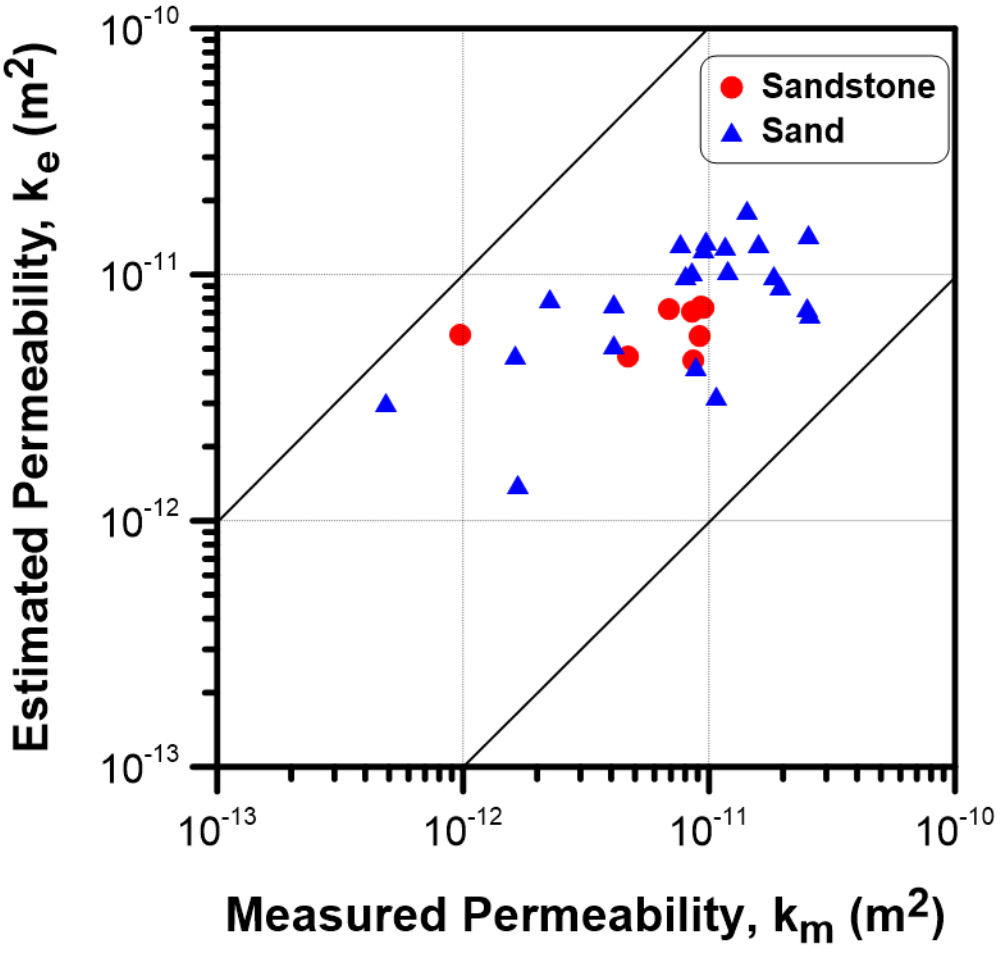

Figure 10. The relationship between measured and predicted permeability using the resistivity model proposed by Purvance and Andricevic (2000).

206x196mm (96 x 96 DPI)